Journal of Power Sources 208 (2012) 271–275

Contents lists available at SciVerse ScienceDirect

Journal of Power Sources

journal homepage: www.elsevier.com/locate/jpowsour

Short communication

Application of quasi-solid-state silica nanoparticles–ionic liquid composite electrolytes to all-solid-state lithium secondary battery

Seitaro Ito, Atsushi Unemoto, Hideyuki Ogawa, Takaaki Tomai, Itaru Honma*

Institute of Multidisciplinary Research for Advanced Materials, Tohoku University, Sendai 980-8577, Japan

ARTICLE INFO

Article history:
Received 2 December 2011
Received in revised form 6 February 2012
Accepted 15 February 2012
Available online 23 February 2012

Keywords:
Lithium
Secondary battery
All solid state
Silica
Ionic liquid

ABSTRACT

Even though the use of solid-state electrolytes for all-solid-state lithium battery applications has been a topic of great interest, an optimal material for this purpose has not been found. On the basis of the fact that ionic liquids are solidified at oxide particle surfaces and become quasi-solid materials, we previously fabricated a new lithium-ion-conducting solid electrolyte material comprising silica nano-particles and an ionic liquid that exhibited high ion conductivity comparable to the bulk ionic liquid. In the current study, this electrolyte was applied in the fabrication of an all-solid-state lithium secondary battery cell, by using three-dimensional structural cathode mixing the solid electrolyte and a cathode material ($LiCoO_2$). The most important feature of the newly developed cell is that it was fabricated using thick films. There are no prior reports of all-solid-state secondary batteries employing thick films that exhibit high capacity. In this design, all of the cathode active materials could make contact with the electrolyte and the electron-conducting material despite the all-solid-state nature of the device. As a result, we have succeeded in the fabrication of an all-solid-state lithium secondary battery exhibiting high capacity of 126 mAh g^{-1}, nearly equal to theoretical capacity 138 mAh g^{-1}, despite the use of a micrometer order thick-film device. This study paves the way for the application of a new approach to the all-solid-state lithium secondary battery design.

1. Introduction

Lithium secondary batteries are promising energy devices for large-scale application in electric vehicles and load leveling [1,2]. Typical lithium ion secondary batteries are constructed with an anode (graphite), a cathode ($LiCoO_2$, $LiFePO_4$), and an organic liquid electrolyte. However, in recent years, the all-solid-state lithium secondary battery that employs the lithium metal as the anode and a solid electrolyte has been considered to be more stable and possesses a high potential for large-scale industrial applications such as in electric vehicles or other renewable energy systems because a lithium metal anode has high theoretical capacity (3860 mAh g^{-1}) compared with a graphite anode (372 mAh g^{-1}). However, the preparation of a solid electrolyte combining the properties of high ion conductivity and resistance for lithium potential reduction is a challenging task. Although several solid-state polymer electrolytes, such as polyethylene oxide [3,4], and inorganic solid electrolyte [5,6], have been investigated for device application, there are still some problems remaining, the stability for lithium metal and low ion conductivity [4,5]. The development of solid-state ion-conducting materials opens up a wider choice of functional materials for lithium secondary battery design and improved performances.

Ionic liquids (ILs) are liquid-state organic salts. ILs have garnered active interest because of their superior properties, such as flame resistance, very low vapor pressure, and high ion conductivity [7,8]. On the basis of these properties, ILs have been explored as new electrolytes for use in the lithium battery [9–11]. Recently, an IL stabilized on an oxide particle surfaces was reported [12–15]. This composite and other such materials have come under the spotlight as a new type of solid-state electrolyte owing to the high ion conductivity, comparable to the bulk IL, exhibited by these materials despite their quasi-solid state. Previously, we reported the solidification of several ILs on oxide particles [16,17], along with the ion-transport properties of the composite materials comprising oxide and the lithium ion conducting IL, lithium bis(trifluoromethanesulfonyl) amide (Li-TFSA) dissolved 1-ethyl-3-methylimidazolium bis(trifluoromethanesulfonyl) amide (EMI-TFSA) [18]. This electrolyte comprises oxide particles coated by a layer of IL, and the ion species conduct along this IL layer (Fig. 1). This series of studies showed that the quasi-solidified composite materials had ion conductivities that were sufficiently high for application as solid electrolytes. In this study, we fabricated an

* Corresponding author at: 2-1-1 Katahira, Aoba-ku, Sendai 980-8577, Miyagi, Japan. Tel.: +81 22 217 5815; fax: +81 22 217 5828.
E-mail addresses: sito@tagen.tohoku.ac.jp (S. Ito), unemoto@tagen.tohoku.ac.jp (A. Unemoto), hideyuki@mail.tagen.tohoku.ac.jp (H. Ogawa), tomai@tagen.tohoku.ac.jp (T. Tomai), i.honma@tagen.tohoku.ac.jp (I. Honma).

0378-7753/$ – see front matter © 2012 Elsevier B.V. All rights reserved.
doi:10.1016/j.jpowsour.2012.02.049

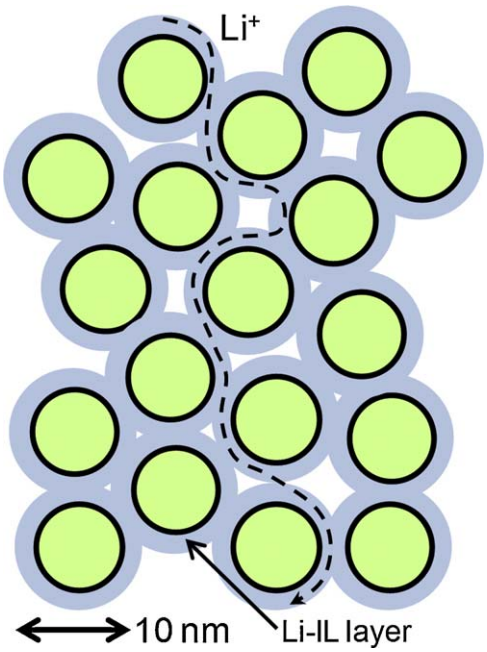

Fig. 1. Conceptual diagram of nano-scale oxide particles (clear-cut inner circles) and ionic liquid (vaguely-outlined outer circles) composite material. Dashed line represents a lithium-ion conduction path.

all-solid-state lithium secondary battery cell using the previously developed composite solid electrolyte comprising silica nanoparticles and the IL (EMI-TFSA) and evaluated the charge–discharge performance of the fabricated battery.

2. Experimental

2.1. Material synthesis

The IL, EMI-TFSA, was purchased from Kanto Kagaku. Li-TFSA powder was purchased by Kishida Kagaku. Fumed silica, Li metal for the anode, and $LiCoO_2$ for the cathode were purchased from Aldrich. Acetylene black (AB, Denka FX35), used as the electron-conducting material, was kindly provided by DENKA. Polyterafluoroethylene (PTFE, PTFE 6-J) was kindly provided by Du-pont Mitsui Fluorochemicals. Li-TFSA was dissolved in EMI-TFSA at a 1 mol L^{-1} Li^+ concentration (1 M Li^+ EMI-TFSA, hereafter referred to as Li-IL). The solid electrolyte was prepared according to our previously reported method [19]. In this study, we prepared the solid electrolyte containing 75 vol% of Li-IL, and the solid electrolyte was pressed into pellets with diameters of 5.0 mm and 0.5 mm height at a pressure 20 MPa. Furthermore, these solid electrolyte pellets were degassed under vacuum at 70 °C to optimize the Li-IL volume ratio. The cathode composite material comprised a mixture of $LiCoO_2$ as an active material, acetylene black (AB) as an electron-conducting material, and PTFE as a binder, with a $LiCoO_2$:AB:PTFE weight ratio of 75:20:5. The cathode thus fabricated is hereafter referred to as "a standard cathode" and the mixture composed of the standard cathode and 40 vol% of Li-IL is referred to as "a mixed cathode". Furthermore, the mixture comprising the mixed cathode and equivalent amount of the 75 vol% of solid electrolyte powder is termed "a three-dimensional (3D) cathode". In the 3D cathode case, the weight ratio of $LiCoO_2$ was 28.5 wt%. Pellets of each cathode material, having 5.0 mm diameter and 0.1 mm thickness, were fabricated by mixing the materials in a mortar and punching. The coin type two-terminal cell stacked with the cathode material, the solid electrolyte, and Li metal anode was sealed in an argon atmosphere glove box.

2.2. Electrochemical measurement

Charge–discharge measurements of the fabricated all-solid-state secondary battery were performed at 65 °C and a rate of 1/10 C over a voltage range of 3.4–4.2 V using a Hokuto Denko HJ 1001SD8 battery test system. The conductivity of the solid electrolyte bulk and the interface between the electrolyte and active materials was measured over a frequency range of 2×10^6 Hz to 0.1 Hz ac impedance using a set of electroanalytical systems consisting of an electrochemical interface (SI1287, Solatron Analytical) and impedance/gain phase analyzer (SI1260, Solatron Analytical).

2.3. Elemental measurement

Surface morphologies and elemental analysis of the cathode materials were carried out using a scanning electron microscopy (SEM, HITACHI S-4000, 15 kV) and a energy dispersive X-ray spectroscopy (EDX, OXFORD) system, respectively. S and Co elements corresponding to the IL (the TFSA of solid electrolyte), and $LiCoO_2$ respectively, were analyzed.

3. Results and discussion

A photograph of the solid electrolyte pellet after vacuum degassing is shown in Fig. 2. The pellets had a water-like transparent appearance reflective of the high Li-IL volume ratio. The Li-IL volume ratio of the degassed pellet used as the solid electrolyte could be deduced to be between 75 vol% and 90 vol% on the basis of the fact that at 90 vol% volume ratio, the pellet assumes a gel state, as shown in our previous report [19].

In our previous study, we found that the composite materials show high ion conductivity. The ion conductivity of the solid electrolyte at a 75 vol% of Li-IL volume ratio was 3.2×10^{-4}–4.4×10^{-3} S cm^{-1} at 287–348 K [19]. This conductivity was sufficiently high for application as solid electrolytes. However, the composite material must show lithium ion conductivity for application in an all-solid-state lithium secondary battery. Fig. 3 shows the results of ac impedance measurements for the solid 75 vol% Li-IL/fumed silica composite electrolyte pellet sandwiched by stainless (SUS) electrodes and Li electrodes. With the SUS electrodes, the blocking interface resistance was produced. On the other hand, a semi-circular shape was observed when the SUS electrodes

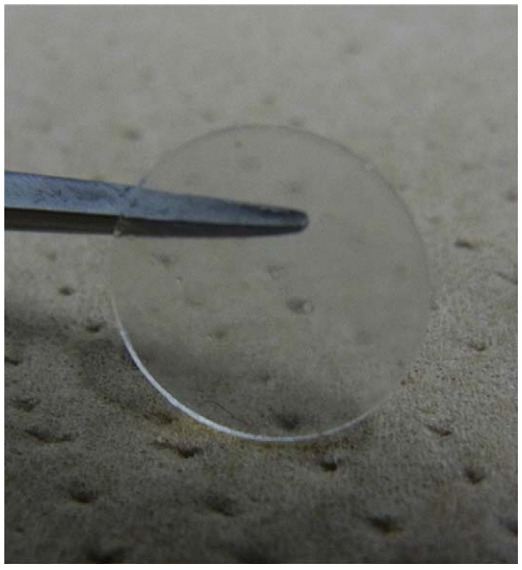

Fig. 2. Photograph of vacuum degassed solid-state electrolyte pellet.

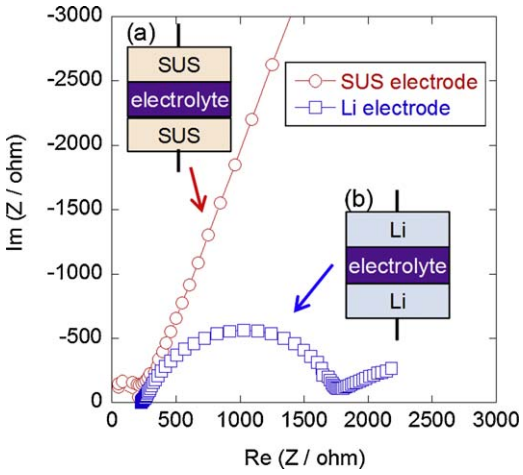

Fig. 3. Cole–Cole plot of ac impedance measurement for 75 vol% Li-IL/fumed silica composite electrolyte sandwiched by (a) SUS electrodes and (b) Li electrodes.

were replaced with Li electrodes. These results indicated that the lithium ion was one of the carrier species in the composite pellet, and thus, this composite material could be applied as the solid-state electrolyte of an all-solid-state lithium battery.

Fig. 4 shows the all-solid-state lithium secondary battery cell structure constructed using the 3D cathode. The quasi-solid state was maintained in the cathode pellet and the solid electrolyte even though they both contained the Li-IL. The thick-film structure (3D cathode: 0.1 mm and solid electrolyte: 0.5 mm) is a quite unique characteristic of the fabricated device. The charge–discharge process for the all-solid-state battery cell constructed using the standard cathode and the mixed cathode was almost instantaneous and the capacity was almost zero. On the other hand, the charge–discharge measurement of the all-solid-state battery cell using the 3D cathode showed a typical curve (Fig. 5) and the capacity values at the first, second and fifth discharge were 126 mAh g^{-1}, 124 mAh g^{-1} and 122 mAh g^{-1} for $LiCoO_2$. Generally, the charge–discharge plateau of the Li anode and the $LiCoO_2$ cathode system appears between 3.8 V and 4.0 V [20]. The charge–discharge plateau of the device fabricated herein also appeared in this region. Therefore, this result indicates that the newly developed hybrid composite material may be suitable as an electrolyte for the lithium secondary battery system. We did not discuss the cycle property in this report. The cycle decay of secondary battery cell consists of Li metal anode, $LiCoO_2$ cathode and EMI-TFSA liquid electrolyte was reported by Sakaebe et al. [9,21]. The cathodic limit of EMI-TFSA was positive against Li/Li^+ potential. They concluded that the cathodic instability of EMI-TFSA was the reason for cycle decay. Charge–discharge measurement of our all-solid secondary battery cell showed the significant cycle decay above 8th cycle (figure not shown here). In addition, silica is not stable against Li in general. Therefore, it is possible that the chemical reaction with silica influences the capacity decay. Investigation into the cause of cycle decay and improvement of cycle property is future task for us.

The theoretical capacity of the $LiCoO_2$ cathode is known to be 138 mAh g^{-1}. The all-solid-state lithium secondary battery cell using the solid electrolyte and the 3D cathode reported herein almost equal to this theoretical capacity of $LiCoO_2$, as shown in Fig. 5. Some secondary battery cells using IL for liquid electrolyte showed high capacity [21,22]. In our previous work, the secondary battery cells using Li-IL for liquid electrolyte showed high capacity, 60 mAh g^{-1} (not shown here). However, there is no report about the all-solid-state "thick-film" secondary battery cell showing high capacity. All-solid-state "thin-film" lithium secondary batteries have demonstrated high capacity. In the thin-film device, a lithium ion can reach all of the $LiCoO_2$ because the micrometer order sized thickness of the cathode film is sufficiently thin for diffusion of the lithium ion. However, lithium-ion diffusion is limited when the thick, bulk-sized cathode is applied to a realistic battery device because the thickness of the cathode is typically in an order of few-tens micrometer scale. Our result is the first report of an all-solid-state lithium secondary battery device employing a thick-film cathode, which exhibits the theoretical capacity. The battery cells with the standard cathode or the mixed cathode showed a capacity almost zero. This result indicates that such a 3D cathode system does not work well in the absence of the fumed silica. Why did only the battery cell using the 3D cathode show high capacity?

The nanoparticulate, powdered nature of this newly developed solid electrolyte offers the advantage of facile preparation of a 3D cathode by mixing cathode active materials. Fig. 6 shows SEM images and EDX mapping of the standard cathode and the 3D cathode surfaces. Some particles including $LiCoO_2$ were observed on the standard cathode surface. The electron-conductor, AB, and the PTFE binder were filled in gaps between the $LiCoO_2$ particles. On the other hand, observation of the 3D cathode surface showed that the materials containing S were filled in gaps between the $LiCoO_2$ particles other than AB and PTFE. S is from the IL (TFSA) of the solid electrolyte. Fig. 6(d) shows that the solid electrolyte was filled in gaps between the $LiCoO_2$ particles, and made contact with the $LiCoO_2$ particles by face contact, and not point contact. Lithium-ion transfer between solid electrolytes and $LiCoO_2$ generally occurs at a point contact interface and its efficiency is very low if the size of the solid electrolyte is comparable to that of $LiCoO_2$ (micrometer order). In the 3D cathode case, however, lithium-ion transfer occurred at a face contact interface and its efficiency was high because the size of solid electrolyte was of the nanometer order. In the standard cathode case, only $LiCoO_2$ particles at the interface could make contact with the solid electrolyte owing to the absence of the solid electrolyte in the cathode film.

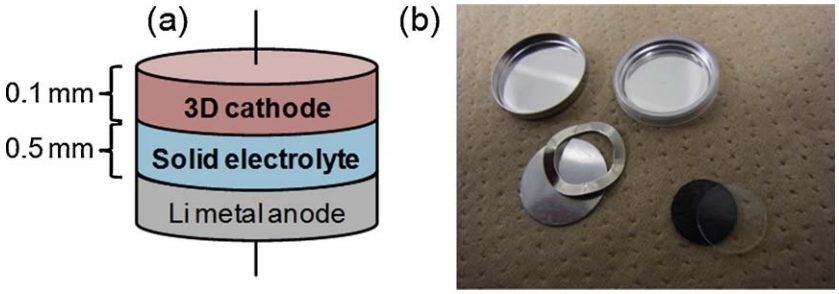

Fig. 4. (a) Device structure of all-solid-state lithium secondary battery fabricated coin cell and (b) the photograph of the coin cell, a solid electrolyte and a 3D cathode (not including lithium metal anode).

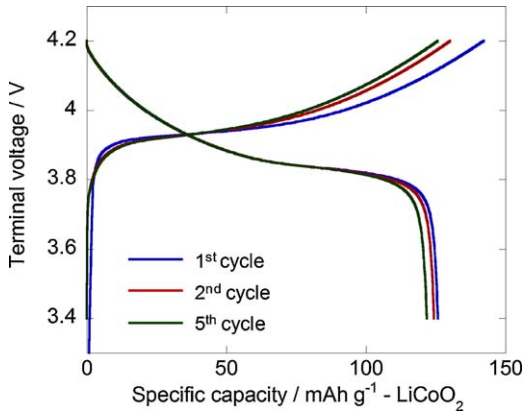

Fig. 5. The first to fifth charge–discharge profiles of all-solid-state secondary lithium battery using the 3D cathode. Charge–discharge measurement was performed at 65 °C and 1/10 C rate. Cut off voltage was from 3.4 V to 4.2 V.

Comparison of the EDX results of the standard cathode and the 3D cathode shows that the 3D cathode device has an advantage conferred by the homogeneous distribution of the solid electrolyte as demonstrated in Fig. 7. In practice, only $LiCoO_2$ particles that can access both AB and the solid electrolyte are able to insert and release lithium ions in the interlayer. A liquid electrolyte readily meets this requirement because the electrolyte can penetrate between the cathode active materials. However, the solid electrolyte could not penetrate between the cathode active materials because of its solid nature. This is an important limitation to solid electrolyte application. In the standard cathode, only $LiCoO_2$ particles at the interface with the solid electrolyte could make contact with the solid electrolyte and the AB. Therefore, most of the $LiCoO_2$ were not activated. On the other hand, almost all of the $LiCoO_2$ in the 3D cathode contacted the solid electrolyte as shown in the EDX results. Therefore, almost all of the $LiCoO_2$ were activated, and the battery cell using the 3D cathode showed high capacity. And the result of the battery cell using the mixed cathode showed that $LiCoO_2$ particles could be activated only by contacting with the solid electrolyte and AB. Contact with the Li-IL and AB is not enough for $LiCoO_2$ activation.

Although it was expected that the mixed cathode was enough for 3-dimensional network formation in cathode pellet, the result was different. We predict that this difference is from wettability between Li-IL and other cathode materials ($LiCoO_2$ or AB). It was observed that the standard cathode pellet repelled a drop of Li-IL. This result indicates the low wettability between Li-IL and other cathode materials. As the result, the 3-dimensional structure with

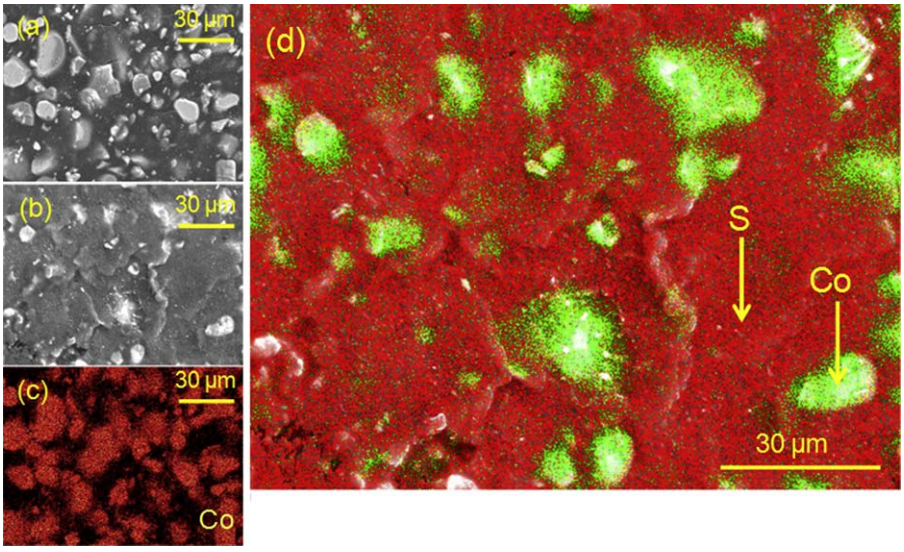

Fig. 6. SEM images of (a) the standard cathode and (b) the 3D cathode. EDX mapping of (c) Co in the standard cathode, (d) Co and S on the 3D cathode surfaces.

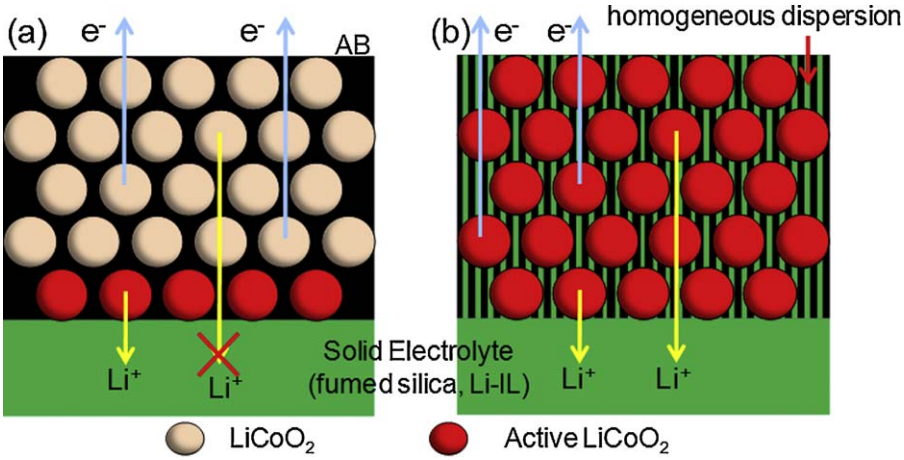

Fig. 7. Conceptual diagram of (a) the interface between the standard cathode and the solid-state electrolyte, and (b) the interface between the 3D cathode and the solid-state electrolyte.

Li-IL and $LiCoO_2$ could not be formed in the mixed cathode. On the other hand, in the case of the 3D cathode, Li-IL and other cathode materials were mixed without repelling. This is because the solidified Li-IL widely dispersed in the cathode materials independently of wettability by silica nano-particle help. As the result, only the 3D cathode device showed theoretical capacity.

4. Conclusion

An all-solid-state secondary battery cell was fabricated using a new solid electrolyte that was previously developed by the current authors [19], and the charge–discharge performance of the fabricated battery was assessed. The battery performance confirmed that the solid electrolyte acts as a high-grade electrolyte. Furthermore, all-solid-state "thick-film" lithium secondary battery cell showing the theoretical capacity was successfully fabricated, combining the solid electrolyte and a 3D cathode. This study demonstrates one possibility for the application of the all-solid-state battery cell and the importance of the structural arrangement of the cell.

Appendix A. Supplementary data

Supplementary data associated with this article can be found, in the online version, at doi:10.1016/j.jpowsour.2012.02.049.

References

[1] B. Scrosati, F. Croce, S. Panero, J. Power Sources 100 (2001) 93–100.
[2] M. Gauthier, D. Fauteux, G. Vassort, A. Belanger, M. Duval, P. Ricoux, J.-M. Chabagno, D. Muller, P. Rigaud, M.B. Armand, D. Deroo, J. Electrochem. Soc. 132 (1985) 1333–1340.
[3] K. Hanai, K. Kusagawa, M. Ueno, T. Kobayashi, N. Imanishi, A. Hirano, Y. Takeda, O. Yamamoto, J. Power Sources 195 (2010) 2956–2960.
[4] D. Saito, Y. Ito, K. Hanai, T. Kobayashi, N. Imahori, A. Hirano, Y. Takeda, O. Yamamoto, J. Power Sources 195 (2010) 6172–6176.
[5] S.D. Jones, J.R. Akridge, F.K. Shokoohi, Solid State Ionics 69 (1994) 357–368.
[6] K. Tanaka, T. Inada, A. Kajiyama, H. Sasaki, S. Kondo, M. Watanebe, M. Murayama, R. Kanno, Solid State Ionics 158 (2003) 269–274.
[7] J. Dupont, R.F. de Souza, P.A.Z. Suarez, Chem. Rev. 102 (2002) 3667–3692.
[8] R.D. Rogers, K.R. Seddon, Science 302 (2003) 792–793.
[9] H. Sakaebe, H. Matsumoto, K. Tatsumi, J. Power Sources 146 (2005) 693–697.
[10] S. Seki, Y. Kobayashi, H. Miyashiro, Y. Ohno, A. Usami, Y. Mita, N. Kihira, M. Watanabe, N. Terada, J. Phys. Chem. B 110 (2006) 10228–10230.
[11] B. Garcia, S. Lavallee, G. Perron, C. Michot, M. Armand, Electrochim. Acta 49 (2004) 4583–4588.
[12] M. Mezger, H. Schoder, H. Reichert, S. Schramm, J.S. Okasinski, S. Schoder, V. Honkimaki, M. Deutsch, B.M. Ocko, J. Ralston, M. Rohwerder, M. Stratmann, H. Dosch, Science 322 (2008) 424–428.
[13] K. Ueno, M. Kasuya, M. Watanabe, M. Mizukami, K. Kurihara, Phys. Chem. Chem. Phys. 12 (2010) 4066–4071.
[14] M-A. Neouze, J.L. Bideau, P. Gaveau, S. Bellayer, A. Vioux, Chem. Mater. 18 (2006) 3931–3936.
[15] T. Watanabe, R. Kawano, M. Watanabe, Electrochem. Solid-State Lett. 10 (2007) F23.
[16] S. Shimano, H. Zhou, I. Honma, Chem. Mater. 19 (2007) 5216–5221.
[17] U.-H. Lee, T. Kudo, I. Honma, Chem. Commun. (2009) 3068–3070.
[18] A. Unemoto, Y. Iwai, S. Mitani, S-W. Baek, S. Ito, T. Tomai, J. Kawamura, I. Honma, Solid State Ionics 201 (2011) 11–20.
[19] A. Unemoto, Y. Iwai, S. Mitani, S.-W. Baek, S. Ito, T. Tomai, J. Kawamura, I. Honma, Abstracts of 18th International Conference on Solid State Ionics, 3–8 July, Warsaw, Poland, 2011, p. 173.
[20] K. Mizushima, P.C. Jones, P.J. Wiseman, J.B. Goodenough, Mater. Res. Bull. 15 (1980) 783–788.
[21] H. Sakaebe, H. Matsumoto, Electrochem. Commun. 5 (2003) 594–598.
[22] M. Ishikawa, T. Sugimoto, M. Kikuta, E. Ishiko, M. Kono, J. Power Sources 162 (2006) 658–662.